Journal of Nuclear Medicine, published on November 16, 2017 as doi:10.2967/jnumed.117.198119

PROstate cancer Molecular Imaging Standardized Evaluation (PROMISE): proposed miTNM classification for the interpretation of PSMA-ligand PET/CT

Matthias Eiber[1,2], Ken Herrmann[1,3], Jeremie Calais[1], Boris Hadaschik[4], Frederik L. Giesel[5], Markus Hartenbach[6], Thomas Hope[7], Robert Reiter[8], Tobias Maurer[9], Wolfgang A. Weber[10], Wolfgang Peter Fendler[1,11,*]

1 Department of Molecular and Medical Pharmacology, David Geffen School of Medicine at UCLA, Los Angeles, CA, USA

2 Department of Nuclear Medicine, Klinikum Rechts der Isar, Technical University of Munich, Germany

3 Klinik für Nuklearmedizin, Universitätsklinikum Essen, Germany

4 Department of Urology, Universitätsklinikum Essen, Germany

5 Department of Nuclear Medicine, University Hospital Heidelberg and DKFZ Heidelberg, Germany

6 Division of Nuclear Medicine, Department of Biomedical Imaging and Image-guided Therapy, Medical University of Vienna, Vienna, Austria

7 Department of Radiology and Biomedical Imaging, University of California, San Francisco, San Francisco, CA, USA

8 Department of Urology, David Geffen School of Medicine at UCLA, Los Angeles, CA, USA

9 Department of Urology, Klinikum Rechts der Isar, Technical University of Munich, Germany

10 Molecular Imaging and Therapy Service, Department of Radiology, Memorial Sloan Kettering Cancer Center, New York, NY

11 Department of Nuclear Medicine, Ludwig-Maximilians-University of Munich, Germany

***Correspondence** should be addressed to Wolfgang Peter Fendler, M.D.; University of California at Los Angeles, Ahmanson Translational Imaging Division, 10833 Le Conte Ave, 200 Medical Plaza, Los Angeles, CA, USA, E-mail: wfendler@mednet.ucla.edu

First author: Matthias Eiber, M.D.; University of California at Los Angeles, Ahmanson Translational Imaging Division, 10833 Le Conte Ave, 200 Medical Plaza, Los Angeles, CA, USA, E-mail: meiber@mednet.ucla.edu

Short title: miTNM for PSMA-ligand PET/CT

Word count:

Key words: PROMISE, miTNM, PSMA-ligand PET/CT, standardized evaluation, interpretation, criteria, miPSMA score

ABSTRACT

Prostate-specific membrane antigen (PSMA)-ligand positron emission tomography (PET)-imaging provides unprecedented accuracy for whole body staging of prostate cancer. As PSMA-ligand PET/computed tomography (CT) is increasingly adopted in clinical trials and routine practice worldwide, a unified language for image reporting is urgently needed. We propose a molecular imaging tumor, node and metastasis system (miTNM Version 1.0) as standardized reporting framework for PSMA-ligand PET/CT or PET/magnetic resonance imaging (MRI). miTNM is designed to organize findings in comprehensible categories to promote exchange of information among physicians and institutions. Additional flowcharts integrating findings of PSMA-ligand PET and morphological imaging were designed to guide image interpretation. Specific applications, such as assessment of prognosis or impact on management, should be evaluated in future trials. miTNM is a “living” framework that evolves with clinical experience and scientific data.

INTRODUCTION

PSMA-ligand PET/CT or PSMA-ligand PET/MRI provides high sensitivity and specificity for prostate cancer staging (*1*). The accuracy of PSMA-ligand hybrid imaging is superior to conventional imaging and tracers such as choline across a range of indications and disease extents (*2-15*). Level 2b evidence for superior detection rates at early biochemical recurrence after radical prostatectomy led to a grade A recommendation for PSMA-ligand PET/CT by the European Association of Urology (*16*). We anticipate increased adoption of PSMA-ligand PET/CT fueled by upcoming evidence and inclusion into guidelines. Thus, reporting standards must be created now to aid reproducibility, enhance communication and ultimately support acceptance of this technology to the benefit of prostate cancer patients.

The PROstate cancer Molecular Imaging Standardized Evaluation (PROMISE) criteria reported in this issue of the Journal of Nuclear Medicine summarize standards for study design and reporting of prostate cancer molecular imaging. We acknowledge that performance characteristics from different studies can only be compared if target regions are properly described and uniformly used. Therefore PROMISE recommends definition of anatomic regions be guided by reproducibility, general applicability, and clinical relevance. Uniform frameworks for image reporting have previously been proposed for pelvic multiparametric MRI (*17*), bone scintigraphy (*18*) and many other techniques and indications (*19,20*). Precise description and organized classification of PSMA-ligand PET/CT findings are needed to serve a number of related subjects:

For clinical reporting:

- Aid clinician in defining tumor extent
- Support clinician in tailoring subsequent therapy management
- Help clinician in assessing prognosis
- Facilitate the exchange of information between centers

For research:

- Aid validation of findings
- Support data pooling within multicenter trials
- Enable meta-analysis of published data

The American Joint Committee on Cancer / Union Internationale Contre le Cancer clinicopathologic tumor, node and metastasis (TNM) system is the most widely used prostate cancer staging system (*21*). In clinical practice TNM is based on a patchwork of information: Local, nodal and distant involvement are categorized by histopathology after surgery or other tissue sampling, as well as clinical findings and imaging. Combination of all modalities improves staging, as each single modality comes with limitations: In prostate cancer clinical examination, ultrasound, CT and MRI demonstrate low sensitivity for metastases (*22*); surgery or biopsy with subsequent histopathology can only evaluate the dissected tissue, thus often underdiagnose prostate cancer metastases at extrapelvic regions or locations outside the operating/sampling field (*23*).

Detection of prostate cancer with PSMA-ligand PET/CT depends on target expression. Based on the high and specific target expression level on most prostate cancer cells, PSMA-ligand PET/CT detects more than half of lymph node metastases with a short diameter ≥2.3 mm and more than 90% of lesions with a short diameter of ≥4.5 mm in a salvage lymphadenectomy setting (*24*). Staging is provided for the entire field of view, also for regions otherwise inaccessible by surgery or biopsy. Based on these unique characteristics, we propose a molecular imaging TNM (miTNM) framework for PSMA-ligand PET/CT prostate cancer staging. This framework may also be applied for PSMA-ligand PET/MRI, single-photon emission computed tomography/CT or similar approaches. miTNM serves standardized reporting of:

- Presence, location and extent of local prostate cancer and its pelvic spread.
- Presence, location, extent and distribution pattern of extrapelvic metastases.
- PSMA expression level of tumor lesions.
- Diagnostic confidence of reported findings.

To support acceptance, implementation and correlation, definitions for the PSMA-ligand PET/CT miTNM framework were designed in analogy to clinicopathologic TNM when possible. Categories were added that describe PSMA expression level and pattern of bone involvement that may e.g. aid planning PSMA-directed therapy or estimating patient prognosis.

PSMA-ligand PET/CT provides high accuracy at substantial to almost-perfect reproducibility for TNM staging among reader with various levels of experience (*25*). Precise and reproducible staging was achieved even without detailed criteria for lesion positivity (*25*). Nevertheless criteria for interpretation (*26-28*) and conduction of PSMA-ligand PET/CT as recently recommended in the joint EANM and SNMMI guideline (*27*) are crucial for successful application of miTNM in prostate cancer staging. Therefore flow charts on morphologic and PSMA-ligand PET findings were designed to guide standardized image interpretation.

An overview of miTNM version 1.0 is given in Tables 1 through 6 and Figures 1 through 4. Anatomic regions and disease patterns are detailed in the following sections.

PSMA expression score and interpretation criteria

A. Rationale

PSMA expression based on immunohistochemistry is known to correlate with tumor differentiation as well as prognosis (*29-31*). Loss of PSMA expression in metastases can indicate de-differentiation and increasing tumor heterogeneity leading to more aggressive phenotypes and a non-response to PSMA-directed therapy (*32,33*). In intraprostatic lesions PSMA-ligand PET has shown to correlate with tumor aggressiveness defined by Gleason Score (*6,34*). Absent PSMA expression measured by PET in a primary tumor raises concerns about missing PSMA-expression in its metastases and therefore provides important advice for interpretation of PSMA-ligand PET

results (*5,35*). Thus, information derived from non-invasive mapping of tumoral PSMA-expression contains valuable information that should be reported for clinical and research PSMA-ligand PET.

B. miPSMA score

We propose a miPSMA score that enables standardized reporting of PSMA expression as detected with PSMA-ligand PET. Expression categories were defined in relation to mean uptake in blood pool, liver and parotid gland (Table 1, Figure 1). Results are reported 0, 1, 2, 3 for no, low, intermediate or high level of PSMA expression, respectively. Scores 2 and 3 are empirically considered typical for prostate cancer lesions and favorable for PSMA-directed radioligand therapy. Expression level will be determined visually and we do not recommend uptake measurements on a regular basis. Occasionally quantitative analyses might be necessary to correctly assign a specific miPSMA score.

Based on personal experience we advise to compare the mean SUVs of the respective lesions and the reference organ. Measurements may be conducted as follows: liver by a 3 cm diameter circular ROI placed in the normal inferior right liver lobe in axial plane; blood pool by a 2 cm diameter circular ROI placed in the center of the aortic arch in axial plane; parotid gland by a 1.5 cm diameter circular ROI placed in the center of the right parotid gland in axial plane; tumor lesion by a 1 cm diameter circular ROI centered over the voxel with maximum uptake in axial plane. Notably, SUV measurements in PSMA-ligand PET requires further validation and investigation to clarify whether SUVmean, SUVmax or peak SUV is the most appropriate parameter.

Detailed data on biodistribution comparing different PSMA-ligands is missing. However application of this score for different PSMA-ligands appears feasible as biodistribution is grossly similar (Figure 1). Known differences in the biodistribution (e.g. higher blood pool activity for ^{18}F-DCFBC or higher liver uptake of ^{18}F-PSMA1007) should be taken into account, especially when comparing studies using different ligands. For PSMA-ligands with liver dominant excretion (e.g. ^{18}F-

PSMA1007) the spleen is recommended instead of the liver for comparison against blood pool and salivary gland uptake (*36*).

C. Interpretation

We want to emphasize that the miPSMA score alone not suitable for diagnosing or excluding prostate cancer. Interpretation of miPSMA scores has to be performed within the clinical context and other imaging findings and in its information can vary for different tissue classes and even locations. A guide for the interpretation of PSMA-directed imaging based on CT, MRI and PET findings is given in Figure 2. Flowcharts were designed based on the authors' clinical experience. However interpretation critically depends on multiple factors including indication, current therapy, PSA and prior clinical, imaging or histopathology findings. Criteria in Figure 2 are not to be taken as absolute definition for positive, negative or equivocal findings. Especially in patients with rising, yet low PSA and otherwise unremarkable imaging findings, even faint but focal uptake above background at typical location may serve as indicator of prostate cancer. Its usability and potential further adoption is prone to prospective clinical validation. Definition of more detailed criteria for certain clinical situation as e.g. recently proposed using consensus reading with multiple Delphi rounds (*28*) is recommended.

The miPSMA score may become useful for patient selection for targeted radiotherapy. At restaging, decrease in miPSMA score in conjunction with morphologic findings can help to identify dedifferentiation or response to therapy.

Final diagnosis and certainty

The final diagnosis should be ideally either positive or negative for prostate cancer. Equivocal findings should be avoided as much as possible and limited to certain settings, e.g. when other techniques may be able to clarify findings. In addition, we recommend reporting diagnostic certainty based on a 5-point scale (Table 6). Certainty will substantially vary depending

on uptake, location and CT or MRI findings. For instance at biochemical recurrence diagnostic certainty will be substantially higher in case of focal uptake at a common location (e.g. internal iliac lymph node) as compared to an uncommon location (e.g. rib). It is further influenced by the specific clinical scenario when e.g. faint uptake in prostate gland after radiation therapy can often represent physiologic background activity compared to radical prostatectomy in which any faint uptake in the former prostate bed is highly suspicious.

Standardized wording for final diagnosis and level of certainty will improve communication between the reader and the treating physician. Implementation into study protocols will allow identification of ambiguous judgements and potential pitfalls aiding future improvement of PROMISE and miTNM. In the future it is desirable to adjust the different categories with data based on studies using histopathological correlation. This will increase their understanding by corresponding physicians and facilitate potential consequences (e.g. change of management).

Local tumor (T)

Local tumor is categorized based on extent and organ confinement (Table 2, Figure 3A). miT0 describes the absence of local recurrence in the pelvis both after radical prostatectomy as well as radiation therapy. miT2 to T4 categorize tumor extent with prostate in place, both treated or untreated. Local organ confined tumor is defined as miT2u for unifocal and miT2m for multifocal involvement. Extraprostatic extension is classified by three categories, in accordance with clinicopathologic TNM: Limited extraprostatic extension (miT3a); involvement of seminal vesicles (miT3b); infiltration of external sphincter, rectum, bladder, levator muscles, and/or pelvic wall (miT4). Based on the spatial resolution of PET for adequate judgement of extraprostatic extension a combination with appropriate cross sectional imaging is needed. This is best achieved by complementing PSMA-ligand PET with multiparametric MRI either within a hybrid PET/MRI study or as a separate dataset available for image fusion. Notably, to avoid confusion with the clinicopathological TNM-system no miT1 category is introduced as T1 by American Joint

Committee on Cancer/Union Internationale Contre le Cancer defines a tumor on histopathology with no correlation on palpation or any type of imaging.

To describe anatomical distribution of intraprostatic tumor extension and to facilitate straightforward correlation between imaging and histopathology (*6,37*) information of prostate involvement is described on sextant base (Table 3). Sextant segments were chosen to provide information for biopsy, the common method for diagnosing prostate cancer. Preferably, for ultrasound biopsy image fusion techniques are recommended encompassing both cognitive as well as software-based approaches (*38-41*). For traditional sextant segmentation the craniocaudal extent of the prostate is divided into three volumes of equal thickness. Volumes will be separated into left and right of the urethra, so as to obtain left basal (LB), right basal (RB), left mid (LM), right mid (RM), left apical (LA), right apical (RA) segments (*6,42*). We are aware that more detailed descriptions of intraprostatic tumor involvement exist e.g. using the local template provided by Prostate Imaging and Reporting and Data System Version 2 (*17*). However, as this system is intended to provide a system for harmonizing image findings across PET/CT and PET/MRI, the sextant approach is most applicable. Recent outcome data, matched with the pathologic tumor stage indicated that tumor extent on sextant base or seminal vesicle infiltration are valuable prognostic information (*43,44*). Nevertheless, in dedicated studies using PET/MRI technology further discrimination of the prostate gland in peripheral and transition zone is recommended for reporting of intraprostatic tumor spread, e.g. using the template proposed in Prostate Imaging and Reporting and Data System Version 2.

The presence of local recurrence in men after radical prostatectomy is categorized by miTr. Infiltration of pelvic structures should be detailed in the report. Probability of local tumor both after radical prostatectomy and radiation therapy increases with focal uptake, higher miPSMA

in the prostate other than the bladder neck/urethra area, typical appearance of local tumor on MRI (diffusion restriction, contrast enhancement) or circumscribed CT contrast enhancement and/or signs of extraprostatic extension. A guide integrating findings of PSMA-ligand PET and

morphological imaging for local tumor presence after primary treatment and for primary staging/tumor detection is given in Figure 2A and B, respectively. Please note that PI-RADS is only applicable investigating patients with increased PSA-value for tumor detection and therefore it should not be combined with interpretation of PSMA-ligand uptake in the setting of primary local staging after histological confirmation (Figure 2B). PSMA-ligand positive pitfalls such as acute prostatitis and MRI-positive pitfalls such as post-biopsy changes and benign nodules have to be ruled out. Notably, low Gleason pattern tumors and some rare entities as intraductal carcinomas tend to be negative on PSMA-ligand PET.

Pelvic nodes (N)

Pelvic nodal metastases will be categorized into single (miN1a) and multiple (miN1b) involved nodal regions. Clinical data indicate that the number of metastatic lymph nodes in histopathology significantly affect disease progression and survival (e.g. recurrence-free survival at 10 years of >70% vs. 49% for patients with 1 or 2 vs. >5 positive lymph nodes) (*45,46*). In addition, it is generally accepted that histopathological information from extended lymph node dissection provides important information for prognosis (*47*)

PSMA-ligand PET/CT is currently regarded as the most powerful application to provide comprehensive overview of nodal involvement in the entire field of view. However, as it is known to fail to identify very small (<2 mm) lymph nodes, we feel reporting based on traditional surgical templates is appropriate (*24*). This provides anatomical information to facilitate comparison with surgery, histopathology, or other imaging findings based on a standardized template for pelvic lymph node regions (Table 4, Figure 4). This template covers the different regions usually approached when extended lymph node dissection is performed (*23*). The anatomical structures delineating template regions for the pelvis adopted to recent reports are described in Table S1 (*48,49*). Each region is encoded by its initials; bilateral regions by a side (left/right, L/R). Besides prognostic value for extent of disease the specific location of lymph node metastases is critical for

surgery and radiation therapy planning. For instance, the presacral or mesorectal regions as well as the retroperitoneum lie outside the typical surgical field.

Probability of nodal involvement increases with focal uptake, higher miPSMA score but also lesion size, contrast enhancement and location. A guide integrating findings in PSMA-ligand PET and morphological imaging for pelvic N-staging is given in Figure 2C. CT/MRI abnormalities such as regional grouping, loss of fatty hilum, or focal necrosis may serve as additional morphologic criteria. PSMA-ligand positive pitfalls such as focal uptake in coeliac ganglia, in an adjacent ureter, inflammation or lymphedema have to be ruled out (*7,25,50,51*).

Extra pelvic nodes and distant metastases (M)

PSMA-ligand PET/CT detects prostate cancer metastases with superior sensitivity and specificity when compared to conventional imaging (*13-15*). At biochemical recurrence organ involvement can be diagnosed early (*2,8,9*) and the exact pattern of disease can be demonstrated. In accordance with clinicopathologic TNM, distant metastases are separated into three categories: extra pelvic lymph nodes (miM1a); bone metastases (miM1b); organ metastases (miM1c) (Table 2, Figure 3B). Location of miM1a nodes will be categorized based on a standard template (Table 4) into retroperitoneal, supradiaphragmatic or other regions. Other lymph node regions or all affected organs in patients with organ involvement (miM1c) should to be further specified in the final report.

PSMA-ligand PET/CT has shown to be superior to bone scintigraphy in describing the extent of bone involvement (*13*). Bone disease will be sub-categorized by pattern of involvement in unifocal, oligometastastic, disseminated disease and diffuse marrow involvement (Table 5, Figure 3B). Oligometastatic bone involvement is diagnosed in case of three or less bone lesions (*52*). In case of unifocal or oligometastatic disease, involved bones should be specified. We acknowledge that the concept and final definition of oligometastic disease is still under debate and

that e.g. certain authors count all types of metastatic lesions up to a specific threshold (*53*). Pattern of bone involvement can have important implications for prognosis (*52,54*) and management (*53*). For instance unifocal disease may be targetable with curative intent by external-beam radiation therapy and diffuse marrow involvement indicates elevated risk for hematotoxicity after radionuclide therapy (*55-57*).

Probability of bone or organ involvement increases with focal uptake, higher miPSMA score and/or CT/MRI abnormalities. For bone metastases common CT findings include sclerotic, rarely lytic lesions with or without extraosseous extension; common MRI findings include low signal on unenhanced T1 images. A guide integrating findings in PSMA-ligand PET and morphological imaging for M-staging is given in Figure 2D. PSMA-ligand positive pitfalls such post-traumatic rib uptake, or non-prostate cancer related primary malignancies have to be ruled out (*26*). A comprehensive overview on potential pitfalls for PSMA-ligand PET-imaging has been recently published (*51*).

Examples

Figure 5 to 7 provide three examples illustrating the use of miTNM in different clinical scenarios.

Limitations

The aim of miTNM is to create a framework for PSMA-ligand PET reporting. We realize, similar to the first clinicopathologic TNM proposal or to other image classification systems, initial definitions are arbitrary and not supported by strong clinical evidence. We admit that besides our approach to parallel the now extensively validated clinicopathologic TNM, incorporated experience of the authors and supporting evidence, no prognostic validation has been performed for miTNM. The historical development of classification systems for imaging (e.g. Breast Imaging Reporting and Data System, Prostate Imaging and Reporting and Data System, Response Evaluation

Criteria In Solid Tumors, PET Response Criteria in Solid Tumors) demonstrate that after an initial proposal with often limited scientific base further adjustments have been conducted sequentially to optimize applicability and clinical validity. We expect and desire a similar process for the herein presented miTNM system. miTNM shall evolve as more evidence for PSMA-ligand PET/CT and patient outcome become available over time. miTNM remains inclusive for other staging systems focusing on local staging or management decisions.

Currently, there are several different PSMA-ligands in clinical use. As currently comparative data on biodistribution and uptake in tumor lesions are not available, caution is warranted when studies based on application of different PSMA-ligands are matched. Therefore, we highly recommend that the specific PSMA-ligand used for an imaging study should be disclosed and application of the same PSMA-ligands is advised when follow-up imaging is performed. Notably, this proposal focuses on small ligands as antibodies (e.g. J591), minibodies or other larger molecules with affinity to PSMA demonstrate a substantially different biodistribution and currently lack data describing their clinical use (*58*).

Future development

PSMA-ligand PET enables unprecedented delineation of whole body tumor burden based on high target to background expression levels (Figure 8) (*59*). Introduction of tools for whole-body tumor volumetry based on a combination of molecular and morphological techniques might overcome several limitations of solely morphological based criteria, such as RECIST (*60*): Lesions without distinct morphological boundaries, such as bone metastases, can be included in the evaluation. Molecular imaging also offers the potential to acknowledge target expression as part of a quantitative imaging biomarker and lesions can be sub-selected by certain target definitions minimizing potential bias.

Consequently, tumor volume could be assessed directly instead of lesion diameter sums. For PSMA-ligand PET initial attempts have been made by introducing PSMA-derived tumor

volume (PSMA-TV), total lesion PSMA (TL-PSMA) or bone-PET-indices (BPI) (*59,61*). Further advances in the field of software-assisted tumor delineation will help to automatically delineate total tumor volume, total tumor target expression or a combination separately for bone and soft tissue. Prospective clinical evaluation is mandatory to assess their potential for prognosis and response in patients with PSMA-expressing prostate cancer.

Summary

We propose miTNM Version 1.0 as standardized framework for PSMA-ligand PET/CT or PET/MRI reporting. miTNM organizes staging of whole-body prostate cancer by including information on exact location, pattern of disease distribution, PSMA expression and level of certainty. miTNM aims to aid information exchange by unifying clinical and research reporting of PSMA-ligand imaging. Prospective evaluation of miTNM needs to be performed, as well as assessment of its impact on patient prognosis and management.

Acknowledgements

We thank Marie Bieth for contributing a case demonstrating software-algorithm based automatic tumor volume delineation. We thank Torsten Kuwert, Christian Schmidkonz, Thorsten Derlin, Steve Rowe and Michael A. Gorin for contributing images outlining the biodistribution of ^{99m}Tc-MIP1404, ^{68}Ga-PSMA I&T and ^{18}F-DCFPyL.

Research support

W.F. received a scholarship from the German Research Foundation (Deutsche Forschungsgemeinschaft, DFG, grant 807122). J.C. received a grant from by the Fondation ARC pour la recherche sur le cancer (grant n°SAE20160604150). M.E. recieved funding within the SFB 824 (DFG Sonderforschungsbereich 824, Project B11) from the Deutsche Forschungsgemeinschaft, Bonn, Germany.

REFERENCES

1. Perera M, Papa N, Christidis D, et al. Sensitivity, specificity, and predictors of opositive 68Ga-prostate-specific membrane antigen positron emission tomography in advanced prostate cancer: a systematic review and meta-analysis. *Eur Urol.* 2016;70:926-937.

2. Eiber M, Maurer T, Souvatzoglou M, et al. Evaluation of hybrid (68)Ga-PSMA ligand PET/CT in 248 patients with biochemical recurrence after radical prostatectomy. *J Nucl Med.* 2015;56:668-674.

3. Eiber M, Nekolla SG, Maurer T, Weirich G, Wester HJ, Schwaiger M. (68)Ga-PSMA PET/MR with multimodality image analysis for primary prostate cancer. *Abdom Imaging.* 2014;40:1769-1771.

4. Rauscher I, Maurer T, Beer AJ, et al. Value of 68Ga-PSMA HBED-CC PET for the assessment of lymph node metastases in prostate cancer patients with biochemical recurrence: comparison with histopathology after salvage lymphadenectomy. *J Nucl Med.* 2016;57:1713-1719.

5. Maurer T, Gschwend JE, Rauscher I, et al. Diagnostic efficacy of (68)Gallium-PSMA positron emission tomography compared to conventional imaging for lymph node staging of 130 consecutive patients with intermediate to high risk prostate cancer. *J Urol.* 2016;195:1436-1443.

6. Fendler WP, Schmidt DF, Wenter V, et al. 68Ga-PSMA PET/CT Detects the Location and Extent of Primary Prostate Cancer. *J Nucl Med.* 2016;57:1720-1725.

7. Herlemann A, Wenter V, Kretschmer A, et al. 68Ga-PSMA Positron Emission Tomography/Computed Tomography Provides Accurate Staging of Lymph Node Regions Prior to Lymph Node Dissection in Patients with Prostate Cancer. *Eur Urol.* 2016;70:553-557.

8. Afshar-Oromieh A, Avtzi E, Giesel FL, et al. The diagnostic value of PET/CT imaging with the (68)Ga-labelled PSMA ligand HBED-CC in the diagnosis of recurrent prostate cancer. *Eur J Nucl Med Mol Imaging.* 2014;42:197-209.

9. Afshar-Oromieh A, Holland-Letz T, Giesel FL, et al. Diagnostic performance of 68Ga-PSMA-11 (HBED-CC) PET/CT in patients with recurrent prostate cancer: evaluation in 1007 patients. *Eur J Nucl Med Mol Imaging.* 2017;44:1258-1268.

10. Afshar-Oromieh A, Malcher A, Eder M, et al. PET imaging with a [68Ga]gallium-labelled PSMA ligand for the diagnosis of prostate cancer: biodistribution in humans and first evaluation of tumour lesions. *Eur J Nucl Med Mol Imaging.* 2013;40:486-495.

11. Kesch C, Vinsensia M, Radtke JP, et al. Intra-individual comparison of 18F-PSMA-1007-PET/CT, multi-parametric MRI and radical prostatectomy specimen in patients with primary prostate cancer - a retrospective, proof of concept study. *J Nucl Med.* 2017.

12. Giesel FL, Fiedler H, Stefanova M, et al. PSMA PET/CT with Glu-urea-Lys-(Ahx)-[(6)(8)Ga(HBED-CC)] versus 3D CT volumetric lymph node assessment in recurrent prostate cancer. *Eur J Nucl Med Mol Imaging.* 2015;42:1794-1800.

13. Pyka T, Okamoto S, Dahlbender M, et al. Comparison of bone scintigraphy and 68Ga-PSMA PET for skeletal staging in prostate cancer. *Eur J Nucl Med Mol Imaging.* 2016;43:2114-2121.

14. Afshar-Oromieh A, Zechmann CM, Malcher A, et al. Comparison of PET imaging with a (68)Ga-labelled PSMA ligand and (18)F-choline-based PET/CT for the diagnosis of recurrent prostate cancer. *Eur J Nucl Med Mol Imaging.* 2014;41:11-20.

15. Rowe SP, Macura KJ, Mena E, et al. PSMA-Based [(18)F]DCFPyL PET/CT Is Superior to Conventional Imaging for Lesion Detection in Patients with Metastatic Prostate Cancer. *Mol Imaging Biol.* 2016;18:411-419.

16. Urology EAo. Update: Guidelines for imaging in patients with biochemical recurrence. http://uroweb.org/guideline/prostate-cancer/?type=summary-of-changes. Available at. Accessed 6/13, 2017.

17. Barentsz JO, Weinreb JC, Verma S, et al. Synopsis of the PI-RADS v2 Guidelines for Multiparametric Prostate Magnetic Resonance Imaging and Recommendations for Use. *Eur Urol.* 2015;69:41-49.

18. Imbriaco M, Larson SM, Yeung HW, et al. A new parameter for measuring metastatic bone involvement by prostate cancer: the Bone Scan Index. *Clin Cancer Res.* 1998;4:1765-1772.

19. Sedgwick EL, Ebuoma L, Hamame A, et al. BI-RADS update for breast cancer caregivers. *Breast Cancer Res Treat.* 2015;150:243-254.

20. Tessler FN, Middleton WD, Grant EG, et al. ACR Thyroid Imaging, Reporting and Data System (TI-RADS): White Paper of the ACR TI-RADS Committee. *J Am Coll Radiol.* 2017;14:587-595.

21. Cheng L, Montironi R, Bostwick DG, Lopez-Beltran A, Berney DM. Staging of prostate cancer. *Histopathology.* 2012;60:87-117.

22. Hovels AM, Heesakkers RA, Adang EM, et al. The diagnostic accuracy of CT and MRI in the staging of pelvic lymph nodes in patients with prostate cancer: a meta-analysis. *Clin Radiol.* 2008;63:387-395.

23. Heidenreich A, Bastian PJ, Bellmunt J, et al. EAU guidelines on prostate cancer. part 1: screening, diagnosis, and local treatment with curative intent-update 2013. *Eur Urol.* 2013;65:124-137.

24. Jilg CA, Drendel V, Rischke HC, et al. Diagnostic Accuracy of Ga-68-HBED-CC-PSMA-Ligand-PET/CT before Salvage Lymph Node Dissection for Recurrent Prostate Cancer. *Theranostics.* 2017;7:1770-1780.

25. Fendler WP, Calais J, Allen-Auerbach M, et al. 68Ga-PSMA-11 PET/CT interobserver agreement for prostate cancer assessments: an international multicenter prospective study. *J Nucl Med.* 2017.

26. Rauscher I, Maurer T, Fendler WP, Sommer WH, Schwaiger M, Eiber M. (68)Ga-PSMA ligand PET/CT in patients with prostate cancer: How we review and report. *Cancer Imaging.* 2016;16:14.

27. Fendler WP, Eiber M, Beheshti M, et al. 68Ga-PSMA PET/CT: Joint EANM and SNMMI procedure guideline for prostate cancer imaging: version 1.0. *Eur J Nucl Med Mol Imaging.* 2017;44:1014-1024.

28. Fanti S, Minozzi S, Morigi JJ, et al. Development of standardized image interpretation for 68Ga-PSMA PET/CT to detect prostate cancer recurrent lesions. *Eur J Nucl Med Mol Imaging.* 2017.

29. Wright GL, Jr., Grob BM, Haley C, et al. Upregulation of prostate-specific membrane antigen after androgen-deprivation therapy. *Urology.* 1996;48:326-334.

30. Wright GL, Jr., Haley C, Beckett ML, Schellhammer PF. Expression of prostate-specific membrane antigen in normal, benign, and malignant prostate tissues. *Urol Oncol.* 1995;1:18-28.

31. Ross JS, Sheehan CE, Fisher HA, et al. Correlation of primary tumor prostate-specific membrane antigen expression with disease recurrence in prostate cancer. *Clin Cancer Res.* 2003;9:6357-6362.

32. Parimi V, Goyal R, Poropatich K, Yang XJ. Neuroendocrine differentiation of prostate cancer: a review. *Am J Clin Exp Urol.* 2015;2:273-285.

33. Yuan TC, Veeramani S, Lin MF. Neuroendocrine-like prostate cancer cells: neuroendocrine transdifferentiation of prostate adenocarcinoma cells. *Endocr Relat Cancer.* 2007;14:531-547.

34. Koerber SA, Utzinger MT, Kratochwil C, et al. 68Ga-PSMA11-PET/CT in newly diagnosed carcinoma of the prostate: correlation of intraprostatic PSMA uptake with several clinical parameters. *J Nucl Med.* 2017.

35. Budaus L, Leyh-Bannurah SR, Salomon G, et al. Initial Experience of Ga-PSMA PET/CT Imaging in High-risk Prostate Cancer Patients Prior to Radical Prostatectomy. *Eur Urol.* 2015.

36. Giesel FL, Hadaschik B, Cardinale J, et al. F-18 labelled PSMA-1007: biodistribution, radiation dosimetry and histopathological validation of tumor lesions in prostate cancer patients. *Eur J Nucl Med Mol Imaging.* 2016.

37. Weinreb JC, Blume JD, Coakley FV, et al. Prostate cancer: sextant localization at MR imaging and MR spectroscopic imaging before prostatectomy--results of ACRIN prospective multi-institutional clinicopathologic study. *Radiology.* 2009;251:122-133.

38. Zettinig O, Shah A, Hennersperger C, et al. Multimodal image-guided prostate fusion biopsy based on automatic deformable registration. *Int J Comput Assist Radiol Surg.* 2015.

39. Costa DN, Pedrosa I, Donato F, Jr., Roehrborn CG, Rofsky NM. MR Imaging-Transrectal US Fusion for Targeted Prostate Biopsies: Implications for Diagnosis and Clinical Management. *Radiographics.* 2015;35:696-708.

40. Moore CM, Kasivisvanathan V, Eggener S, et al. Standards of reporting for MRI-targeted biopsy studies (START) of the prostate: recommendations from an International Working Group. *Eur Urol.* 2013;64:544-552.

41. Rosenkrantz AB, Verma S, Choyke P, et al. Prostate Magnetic Resonance Imaging and Magnetic Resonance Imaging Targeted Biopsy in Patients with a Prior Negative Biopsy: A Consensus Statement by AUA and SAR. *J Urol.* 2016;196:1613-1618.

42. Eiber M, Weirich G, Holzapfel K, et al. Simultaneous 68Ga-PSMA HBED-CC PET/MRI Improves the Localization of Primary Prostate Cancer. *Eur Urol.* 2016;70:829-836.

43. Salomon L, Colombel M, Patard JJ, Gasman D, Chopin D, Abbou CC. Prostate Biopsy in the staging of prostate cancer. *Prostate Cancer Prostatic Dis.* 2002;1:54-58.

44. Vallancien G, Bochereau G, Wetzel O, Bretheau D, Prapotnich D, Bougaran J. Influence of preoperative positive seminal vesicle biopsy on the staging of prostatic cancer. *J Urol.* 1994;152:1152-1156.

45. Daneshmand S, Quek ML, Stein JP, et al. Prognosis of patients with lymph node positive prostate cancer following radical prostatectomy: long-term results. *J Urol.* 2004;172:2252-2255.

46. Boorjian SA, Thompson RH, Siddiqui S, et al. Long-term outcome after radical prostatectomy for patients with lymph node positive prostate cancer in the prostate specific antigen era. *J Urol.* 2007;178:864-870; discussion 870-861.

47. Budiharto T, Joniau S, Lerut E, et al. Prospective evaluation of 11C-choline positron emission tomography/computed tomography and diffusion-weighted magnetic resonance imaging for the nodal staging of prostate cancer with a high risk of lymph node metastases. *Eur Urol.* 2011;60:125-130.

48. Joniau S, Van den Bergh L, Lerut E, et al. Mapping of pelvic lymph node metastases in prostate cancer. *Eur Urol.* 2012;63:450-458.

49. Nicolau BP, Carmen S, Laura B, et al. Pathways of Lymphatic Spread in Male Urogenital Pelvic Malignancies. *http://dxdoiorg/101148/rg311105072.* 2011.

50. Krohn T, Verburg FA, Pufe T, et al. [(68)Ga]PSMA-HBED uptake mimicking lymph node metastasis in coeliac ganglia: an important pitfall in clinical practice. *Eur J Nucl Med Mol Imaging.* 2014;42:210-214.

51. Sheikhbahaei S, Afshar-Oromieh A, Eiber M, et al. Pearls and pitfalls in clinical interpretation of prostate-specific membrane antigen (PSMA)-targeted PET imaging. *Eur J Nucl Med Mol Imaging.* 2017.

52. Schweizer MT, Zhou XC, Wang H, et al. Metastasis-free survival is associated with overall survival in men with PSA-recurrent prostate cancer treated with deferred androgen deprivation therapy. *Ann Oncol.* 2013;24:2881-2886.

53. Tosoian JJ, Gorin MA, Ross AE, Pienta KJ, Tran PT, Schaeffer EM. Oligometastatic prostate cancer: definitions, clinical outcomes, and treatment considerations. *Nat Rev Urol.* 2016;14:15-25.

54. Ost P, Decaestecker K, Lambert B, et al. Prognostic factors influencing prostate cancer-specific survival in non-castrate patients with metastatic prostate cancer. *Prostate.* 2014;74:297-305.

55. Parker C, Nilsson S, Heinrich D, et al. Alpha emitter radium-223 and survival in metastatic prostate cancer. *N Engl J Med.* 2013;369:213-223.

56. Rahbar K, Ahmadzadehfar H, Kratochwil C, et al. German multicenter study investigating 177Lu-PSMA-617 radioligand therapy in advanced prostate cancer patients. *J Nucl Med.* 2016.

57. Jong JM, Oprea-Lager DE, Hooft L, et al. Radiopharmaceuticals for Palliation of Bone Pain in Patients with Castration-resistant Prostate Cancer Metastatic to Bone: A Systematic Review. *Eur Urol.* 2015;70:416-426.

58. Pandit-Taskar N, O'Donoghue JA, Durack JC, et al. A Phase I/II Study for Analytic Validation of 89Zr-J591 ImmunoPET as a Molecular Imaging Agent for Metastatic Prostate Cancer. *Clin Cancer Res.* 2015;21:5277-5285.

59. Bieth M, Kronke M, Tauber R, et al. Exploring New Multimodal Quantitative Imaging Indices for the Assessment of Osseous Tumour Burden in Prostate Cancer using 68Ga-PSMA-PET/CT. *J Nucl Med.* 2017.

60. Eisenhauer EA, Therasse P, Bogaerts J, et al. New response evaluation criteria in solid tumours: revised RECIST guideline (version 1.1). *Eur J Cancer.* 2008;45:228-247.

61. Schmuck S, von Klot CA, Henkenberens C, et al. Initial Experience with Volumetric 68Ga-PSMA I&T PET/CT for Assessment of Whole-body Tumor Burden as a Quantitative Imaging Biomarker in Patients with Prostate Cancer. *J Nucl Med.* 2017.

FIGURES

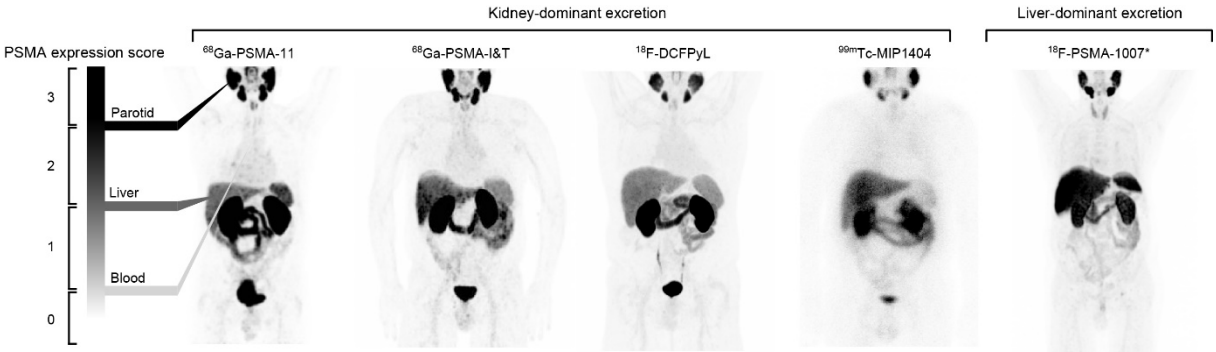

Figure 1: miPSMA expression score. Thresholds are demonstrated on a ^{68}Ga-PSMA11 PET maximum-intensity projection (MIP) image (left). For comparison images are shown for ^{68}Ga-PSMA-I&T, ^{18}F-PSMA-1007, and ^{18}F-DCFPyL MIP one hour and for ^{99m}Tc-MIP1404 planar scan three hours after i.v. application. * For PSMA-ligands with ligands with liver dominant excretion the spleen is recommended as reference organ instead of the liver.

A

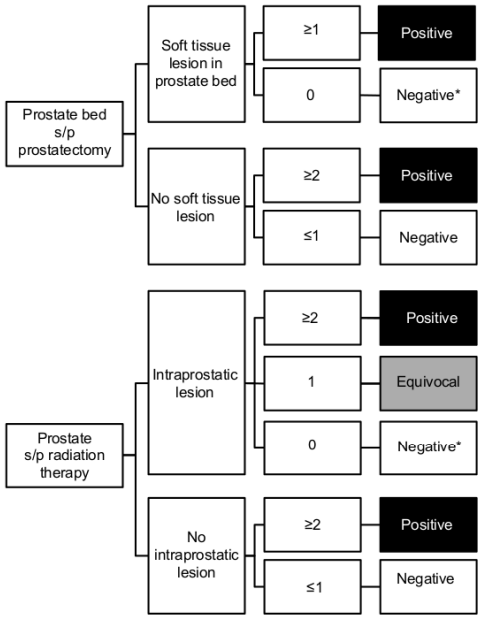

B

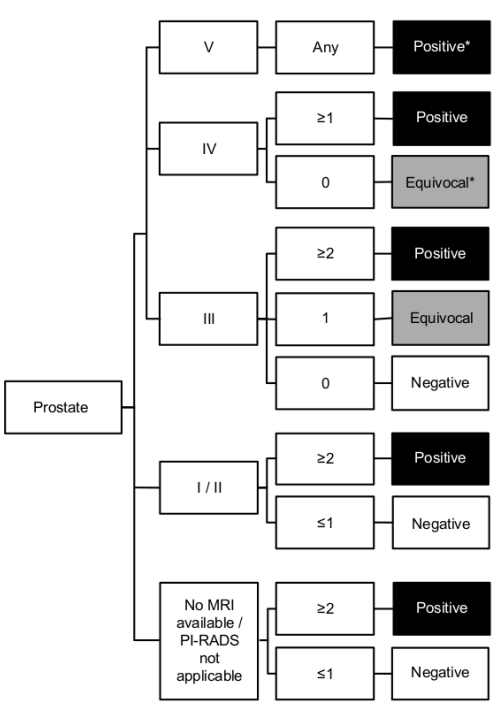

C

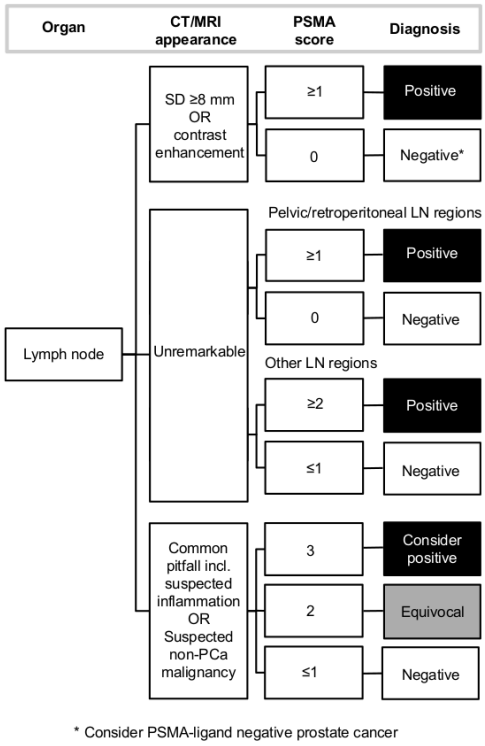

* Consider PSMA-ligand negative prostate cancer

D

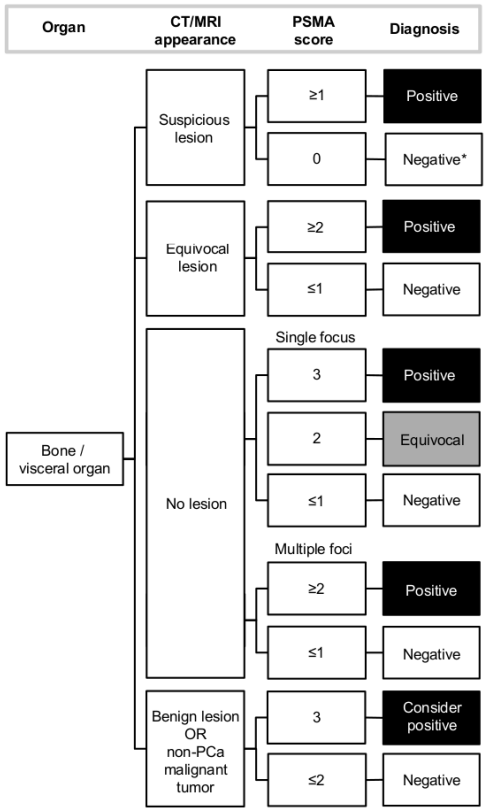

Figure 2: Guide for the interpretation of PSMA-ligand PET/CT or PET/MRI. Criteria are given separately for (A) status post (s/p) prostatectomy or s/p radiation therapy, (B) tumor detection or primary staging of the prostate, (C) lymph nodes, (D) bone or visceral organs. Abbreviation: SD, short axis diameter; LN, lymph node; PIRADS; Prostate Imaging and Reporting and Data System.

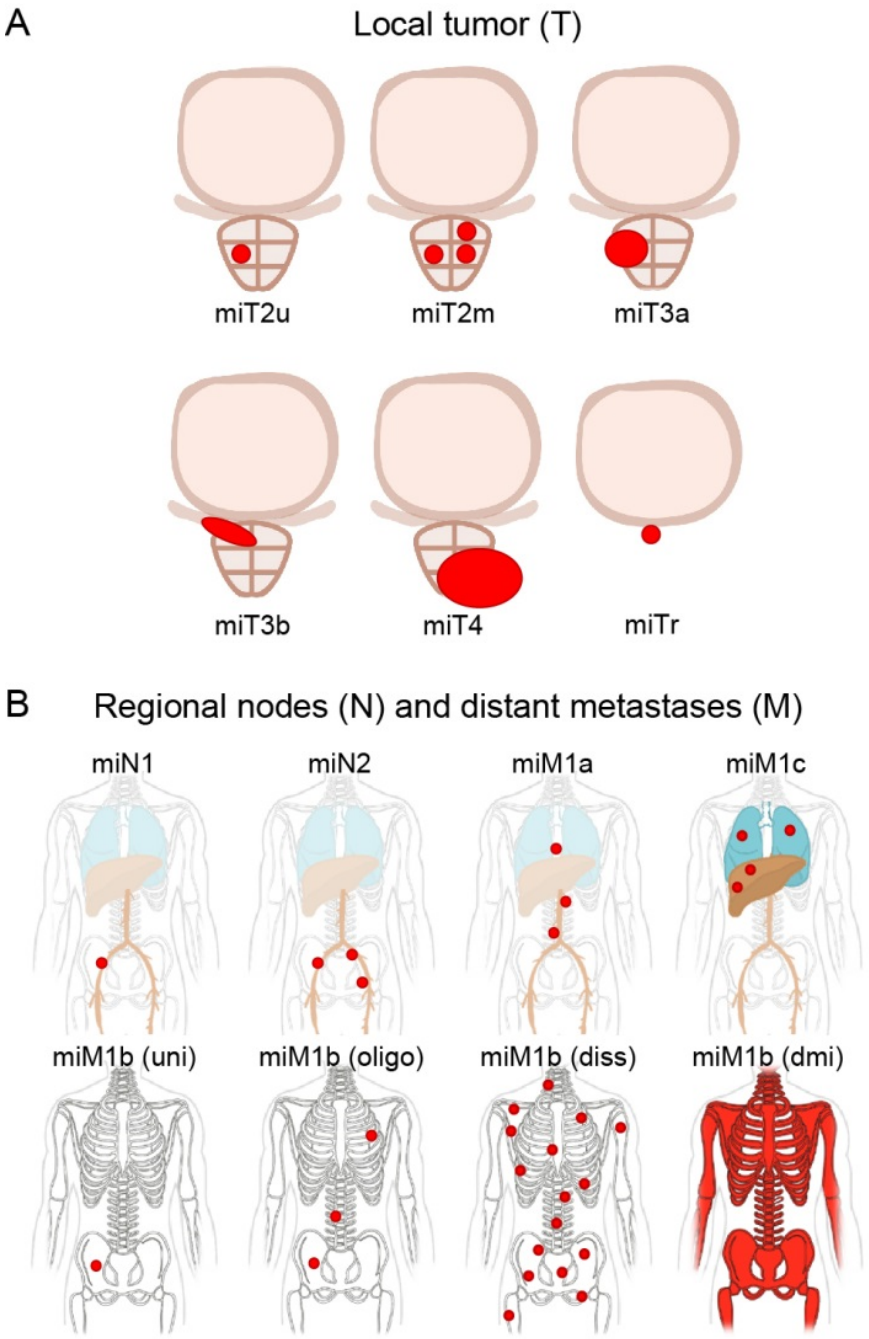

Figure 3: miTNM categories and pattern of bone involvement for reporting prostate cancer stage by PSMA-ligand PET/CT. (A) Local tumor extent. (B) Pelvic nodal and distant metastases. Tumor involvement is delineated in red. Abbreviations: uni, unifocal; oligo, oligometastatic; diss, disseminated; dmi, diffuse marrow involvement.

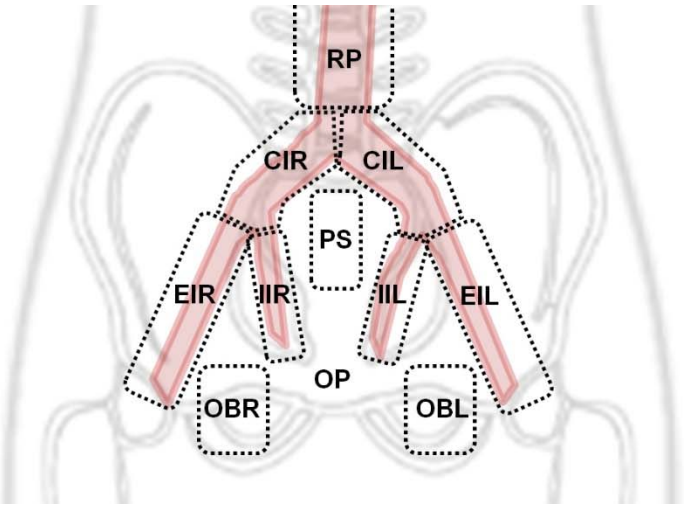

Figure 4: miTNM standard template for pelvic lymph node regions. Transition to the extrapelvic region RP is indicated.

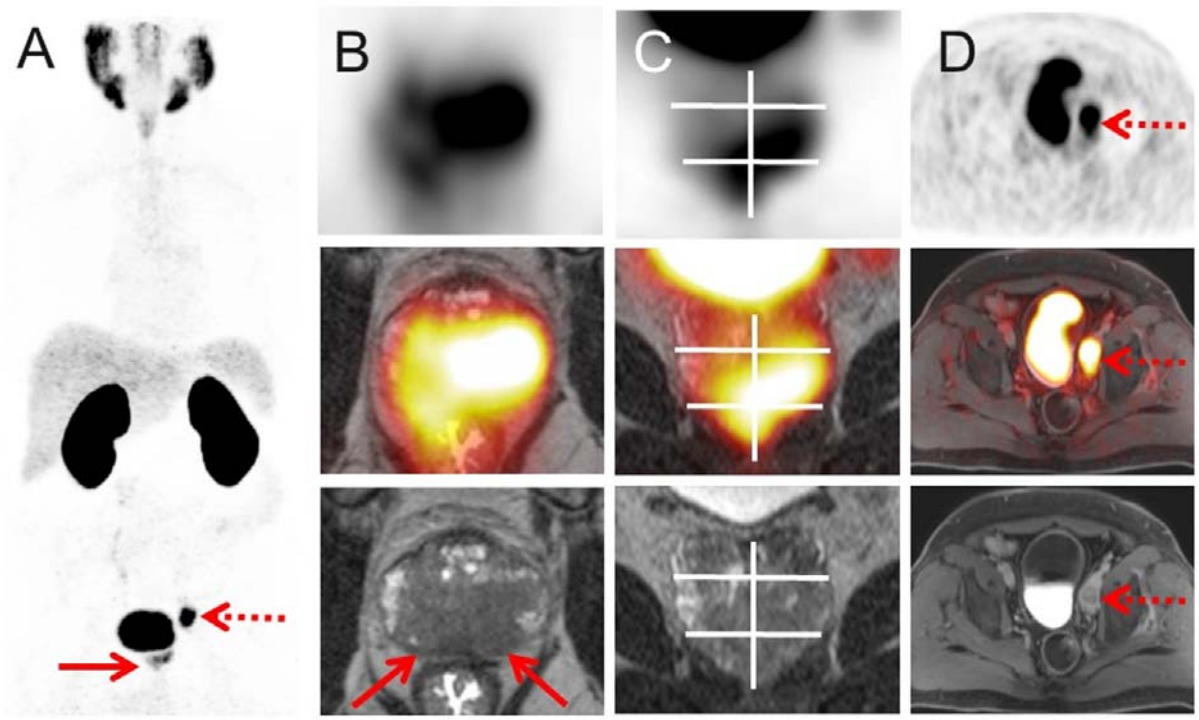

Figure 5: Primary staging using ^{68}Ga-PSMA11 PET/MRI in a 65 y/o patient with histopathologically proven prostate cancer. (A) Maximum-intensity projection PET images demonstrate intermediate (score 2) PSMA expression in the prostate gland (arrow) and high (score 3) PSMA expression for a regional pelvic lymph node (dotted arrow). (B and C) High-resolution T2w MRI images of the prostate demonstrate bilateral T2 hypointense lesions corresponding with uptake in PSMA-ligand PET and clearly exceeding the prostate margins indicative for extraprostatic extension (T3a; arrows). PET/MRI demonstrates bilateral involvement of apical and mid segments and of the left basal segment. Sextant segment boundaries are shown on coronal images in white. (D) Axial images demonstrate a single lymph node metastasis in the left obturator region (IV).

Final diagnosis: miT3a N1 (OBL) M0. All findings were confirmed by post-operative histopathology.

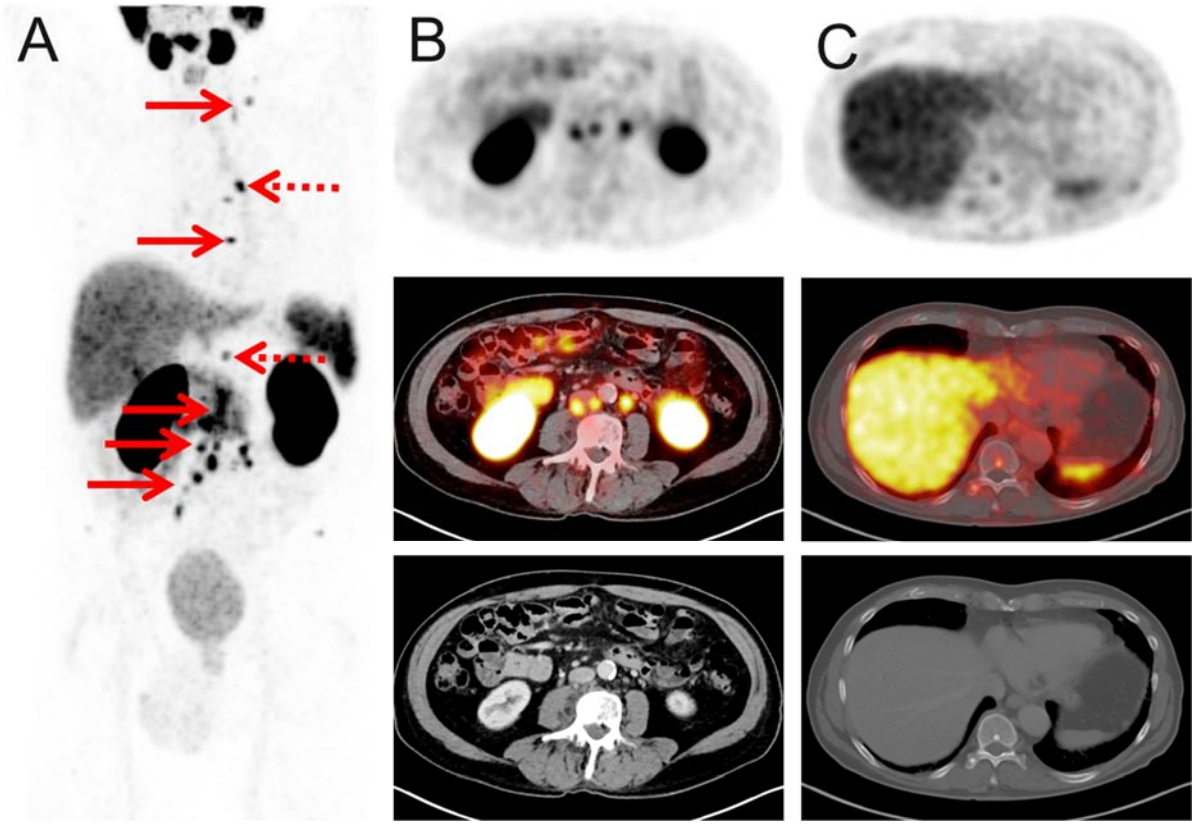

Figure 6. ^{68}Ga-PSMA11 PET/CT restaging in a 62 y/o patient with biochemical recurrent prostate cancer and rising PSA level. (A and B) Maximum-intensity projection PET images demonstrate multiple retroperitoneal as well as supradiaphragmatic lymph node metastases with intermediate (score 2) PSMA expression (arrows). A total of three bone lesions (dotted arrows) define oligometastatic bone involvement. (C) Sclerotic bone metastasis in the thoracic spine demonstrates low (score 1) PSMA expression.

Final diagnosis: miT0 N0 M1a (RP, SD) b (oligo).

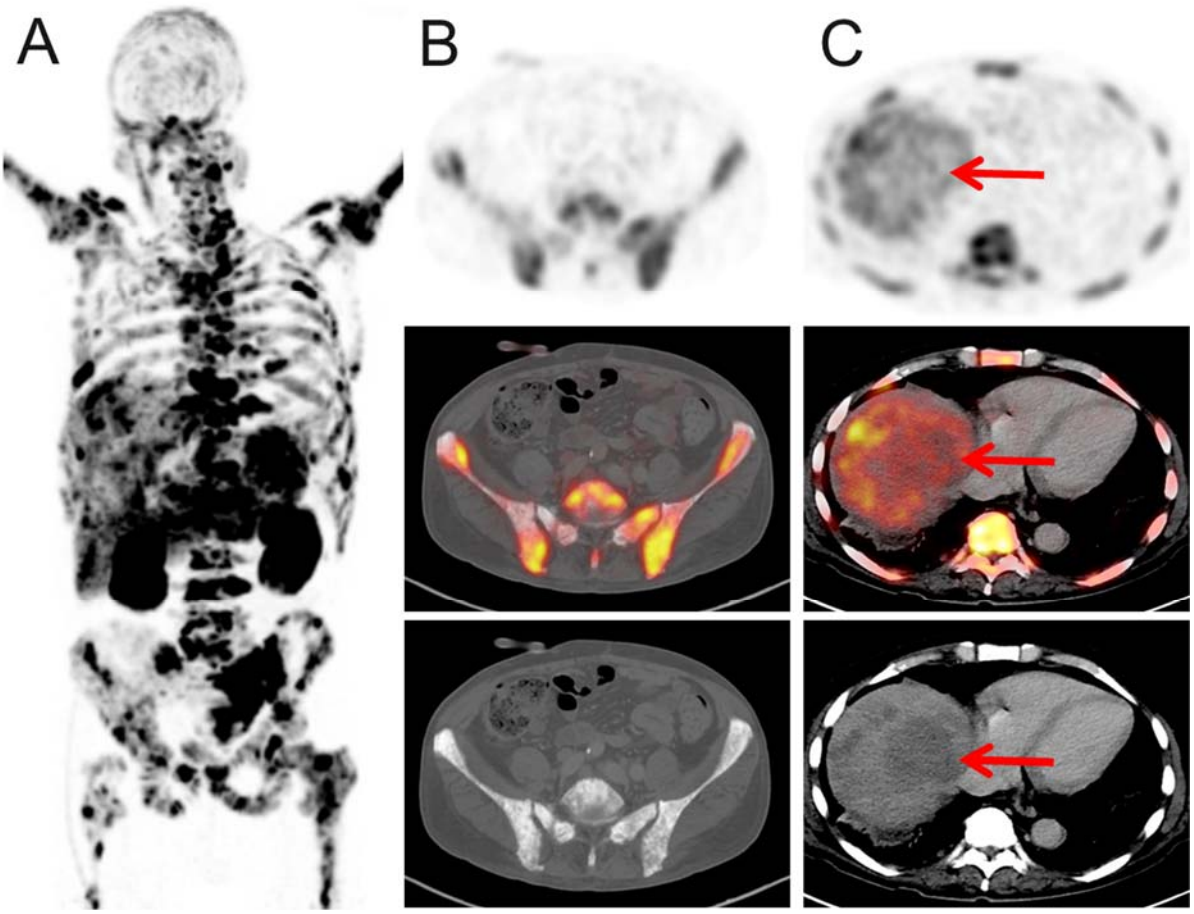

Figure 7. ^{68}Ga-PSMA11 PET/CT restaging in a 76 y/o patient with advanced metastatic castration resistant prostate cancer prior to potential PSMA-radioligand therapy. (A and B) Maximum-intensity projection PET and axial PET/CT images demonstrate diffuse uptake in the skeleton with low to high (score 1 to 3) PSMA expression. (C) Contrast enhanced CT demonstrates multiple liver metastases with low (score 1) PSMA expression.

Final diagnosis: miT0 N0 M1b (dmi) c (liver). PSMA-radioligand therapy was omitted due to diffuse marrow involvement and low PSMA expression in liver metastases.

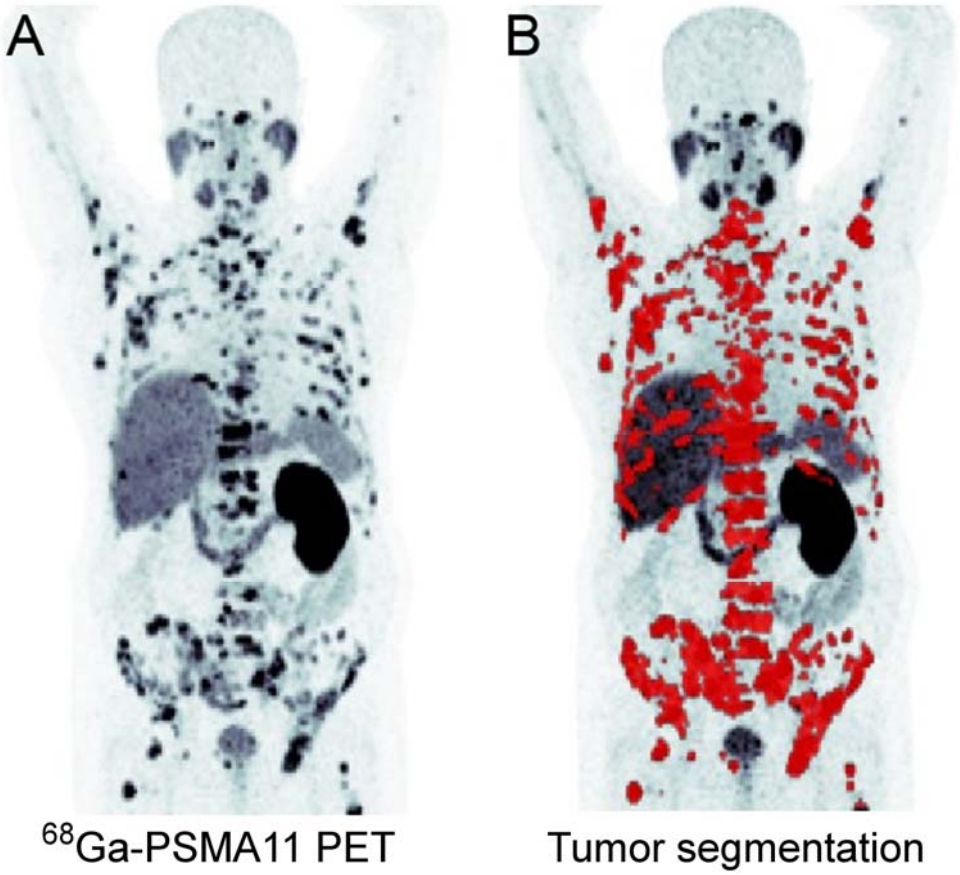

Figure 8: Whole-body prostate cancer volume in a patient s/p radical prostatectomy and second line androgen deprivation therapy. (A) ^{68}Ga-PSMA11 PET maximum-intensity projection demonstrates miT0 N0 M1b (diss) disease. **(B)** Tumor volume was delineated in red using an automatic software-algorithm as recently published (*59*).

TABLES

Score	Reported PSMA expression	Uptake
0	no	Below bloodpool
1	low	Equal to or above bloodpool and lower than liver*
2	intermediate	Equal to or above liver* and lower than parotid gland
3	high	Equal to or above parotid gland

Table 1: miPSMA expression score.
***** for PSMA-ligands with ligands with liver dominant excretion (e.g. ^{18}F-PSMA1007) the spleen is recommended as reference organ instead of the liver

Local tumor (T)		
miT0		No local tumor
miT2		Organ confined tumor, report intraprostatic tumor location(s) on sextant base (Table 3).
	u	Unifocality
	m	Multifocality
miT3		Non-organ confined tumor, report intraprostatic tumor location(s) on sextant base (Table 3).
	a	Extracapsular extension
	b	Tumor invades seminal vesicle(s)
miT4		Tumor invades adjacent structures other than seminal vesicles, such as external sphincter, rectum, bladder, levator muscles, and/or pelvic wall.
miTr		Presence of local recurrence after radical prostatectomy
Regional nodes (N)		
miN0		No positive regional lymph nodes
miN1a		Single lymph node region harbors lymph node metastases, report location by a standardized template (Table 4).
miN1b		Multiple (≥2) lymph node regions harbor lymph node metastases, report location(s) by a standardized template (Table 4).
Distant metastases (M)		
miM0		No distant metastasis
miM1		Distant metastasis
	a	Extrapelvic lymph node(s), additionally report location by a standardized miM1a template (Table 4).
	b	Bone(s), additionally report pattern (Table 5) and involved bone(s) in case of unifocal or oligo metastatic
	c	Other site(s), additionally report involved organ.

Table 2: miTNM classification for PSMA-ligand PET/CT or PET/MRI.

Segment	miT2-4 template
LB	Left base
RB	Right base
LM	Left mid
RM	Right mid
LA	Left apex
RA	Right apex

Table 3: Sextant segmentation of prostate gland

Region	miN1a/b template	Report left/right
II	Internal iliac	Yes
EI	External iliac	Yes
CI	Common iliac	Yes
OB	Obturator	Yes
PS	Presacral (aka: presciatic)	No
OP	Other pelvic (specify)	No
	miM1a template	
RP	Retroperitoneal	No
SD	Supradiaphragmatic	Yes or No
OE	Other extra pelvic (specify)	Yes or No

Table 4: Lymph node regions. Details on the anatomic definition of the lymph node regions are provided in Table S1.

Abbreviation	Pattern of bone involvement
uni	Unifocal
oligo	Oligometastatic (n≤3)
diss	Disseminated
dmi	Diffuse marrow involvement

Table 5: Pattern of bone involvement.

Certainty	Diagnosis
Consistent with	positive
Suspicious for	positive
Possible	equivocal
Unlikely	negative
No evidence of disease	negative

Table 6: Certainty and final diagnosis. Final diagnosis should be reported as positive or negative for prostate cancer. Equivocal diagnosis should only be used when alternative techniques are available that may reasonably provide clarification.

miNa/b template	Anatomical boundaries
Internal iliac (II)	bifurcation internal/external iliac arteries, pelvic floor, bladder wall, obturator nerve
External iliac (EI)	bifurcation internal/external iliac arteries, circumflex iliac vein and endopelvic fascia, psoas muscle and genitofemoral nerve and medial border external iliac artery
Common iliac (CI)	aortic bifurcation, bifurcation internal/external iliac arteries, psoas muscle and genitofemoral nerve and medial border common iliac artery
Obturator (OB)	bifurcation internal/external iliac arteries, pelvic floor, obturator nerve, and medial border external iliac artery
Presacral (PS, aka: presciatic)	Triangle between medial borders of common iliac arteries and line connecting internal/external iliac arteries' bifurcations; dorsal border: promontory and proximal sacrum (S1–S2)

Table S1: Description of anatomical delineation of pelvic lymph node territories (adapted from Joniau et al; Nicolau et al.)